

Norcantharidin inhibits the malignant progression of cervical cancer by inducing endoplasmic reticulum stress

ZHONGBAO ZHANG, BEIBEI SUN, JINQIU LU, PENGLAI BAI, YU SU and YANCHUN LI

Department of Gynecology, Tongliao City Hospital, Tongliao, Inner Mongolia Autonomous Region, P.R. China

Received November 26, 2023; Accepted January 30, 2024

DOI: 10.3892/mmr.2024.13195

Abstract. The antitumor effect of norcantharidin (NCTD) has been widely reported. However, whether NCTD can inhibit cervical cancer remains unknown. In the present study, it was shown that NCTD inhibited the viability of cervical cancer cells and caused cell cycle arrest in a concentration-dependent manner. Further analysis revealed that the NCTD-induced reduction in cell viability could be reversed by the inhibitor of apoptosis z-VAD-FMK and by the inhibitor of endoplasmic reticulum (ER) stress, 4-phenylbutyric acid (4-PBA). Additionally, NCTD led to the accumulation of reactive oxygen species as well as a decrease in the mitochondrial membrane potential in cervical cancer cells, whereas 4-PBA pre-treatment attenuated these alterations. In addition, NCTD increased the expression of the apoptosis-related proteins Bip, activating transcription factor (ATF) 4 and C/EBP homologous protein in a concentration-dependent manner. Moreover, NCTD significantly increased the expression of the ER stress-related signaling molecules protein kinase R-like ER kinase, inositol-requiring enzyme 1 and ATF6, but 4-PBA abolished these effects. *In vivo* experiments showed that NCTD significantly inhibited the growth of subcutaneous tumors in mice. Additionally, the expression of ER stress-related molecules and apoptosis-related proteins increased significantly after NCTD treatment. In conclusion, NCTD induces apoptosis by activating ER stress and ultimately curtails the progression of cervical cancer.

Introduction

Cervical cancer is the most common gynecological malignancy and ranks second among female malignancies worldwide (1). The pathogenesis of cervical cancer is complex, and human papilloma virus (HPV) is the main cause of cervical cancer

with ~95% of cervical cancer cases reported to be caused by HPV infection (2). Once HPV infects cervical epidermal cells, the expression of the oncogenes E6 and E7 inactivates p53 and pRb, which ultimately leads to malignant proliferation of cervical cells (2). In addition, factors such as family heredity, obesity and an unhealthy lifestyle are risk factors for cervical cancer (3). In recent years, the incidence of cervical cancer has been gradually increasing, with a trend towards younger women, which has seriously affected the lives of female patients and even led to death (4,5). Therefore, early detection and active prevention of cervical cancer are important research topics for gynecological malignant tumors.

The endoplasmic reticulum (ER) is an organelle in eukaryotic cells that plays an important role in the maintenance of calcium homeostasis, lipid synthesis, and protein folding and modification (6). The homeostasis of the ER is essential for ensuring that proteins are correctly folded, whereas slow-folding or unfolded proteins are retained in the ER and degraded via the proteasome pathway, which is known as the unfolded protein response (UPR) (7). As unfolded proteins accumulate in the ER, ER transmembrane proteins, whose N-termini are in the ER lumen and whose C-termini are in the cytoplasm, connect the ER to the cytoplasm (8). Normally, the N termini of these ER transmembrane proteins are regulated by the ER chaperone protein Grp78 (Bip), which organizes their aggregation (9). However, when unfolded proteins accumulate in the ER, Bip is released, allowing these transmembrane signaling proteins to aggregate and transmit UPR signals (10). Protein kinase R-like ER kinase (PERK), inositol-requiring enzyme 1 (IRE1) and activating transcription factor (ATF) 6 are important molecules in the three ER stress signaling pathways (11). PERK is a serine/threonine protein kinase with a catalytic structural domain that is highly homologous to kinases of the eukaryotic initiation factor 2 α (eIF2 α) family (12). Once Bip is released, PERK begins to oligomerize during ER membrane activation, inducing autophosphorylation and activating the kinase structural domain to an inactivated state, thus blocking the translation of downstream mRNAs and reducing the protein load in the ER (Fig. 1) (12). However, when eIF2 α expression is restricted, several mRNAs, including ATF4, containing open reading frames at the 5' end begin to be translated (13). ATF4 drives transcription factor C/EBP homologous protein (CHOP), which regulates the expression of apoptosis-related genes (13). It is well known that persistent activation of ER stress can

Correspondence to: Dr Zhongbao Zhang, Department of Gynecology, Tongliao City Hospital, 668 Horqin Street, Horqin, Tongliao, Inner Mongolia Autonomous Region, P.R. China
E-mail: zhangzhongbaox@163.com

Key words: norcantharidin, cervical cancer, endoplasmic reticulum stress, apoptosis

directly regulate tumor cell death, including apoptosis, by initiating a variety of related signaling pathways (11).

Cantharidin is a major anticancer component of the traditional Chinese medicine *Zanthoxylum*, but it is highly toxic to the urinary system (14). Norcantharidin (NCTD) is a novel compound formed by removing two methyl groups on the basis of cantharidin, and the former significantly reduces the side effects of the latter; this compound has been widely used in the clinic (14). The antitumor effects of NCTD have been widely reported (15,16). For example, in bladder cancer cells, NCTD inhibited the malignant proliferation of bladder cancer stem cell-like cells by targeting CDC6 (16). In non-small cell lung cancer types, NCTD induces cell death in a mitophagy-dependent manner (15). However, whether NCTD inhibits cervical cancer has not been reported. The aim of the present study was to investigate whether NCTD inhibits the malignant progression of cervical cancer and the underlying molecular mechanism through the discovery of new effective drugs for the early prevention and treatment of cervical cancer.

Materials and methods

Cell culture. The human cervical cancer cell lines C-33A and HeLa were purchased from Procell Life Science & Technology Co., Ltd. C-33A and HeLa cells were cultured in MEM (HyClone; Cytiva) supplemented with 10% fetal bovine serum (HyClone; Cytiva) in an incubator at 37°C with 5% CO₂.

Western blotting. A total of 100 mg of tumor tissue and cervical cancer cells were collected, RIPA buffer (high; Beijing Solarbio Science & Technology Co., Ltd.) was added, and the samples were centrifuged at 10,000 x g for 15 min at room temperature to collect the supernatant. Subsequently, a BCA protein assay kit (Beijing Solarbio Science & Technology Co., Ltd.) was used to measure the protein concentration in the supernatants. In the present study, 10% SDS-PAGE was used to separate the protein samples (20 µg/lane). After electrophoresis, the proteins were transferred to a PVDF membrane (Thermo Fisher Scientific, Inc.). After which, the PVDF membrane was rinsed with PBST (PBS supplemented with 0.1% Tween-20, Beijing Solarbio Science & Technology Co., Ltd.) and blocked with 8% skim milk (Thermo Fisher Scientific, Inc.) at room temperature for 2 h. After the PVDF membranes were rinsed, they were incubated with the following primary antibodies: Anti-ATF4 (cat. no. 11815), anti-CHOP (cat. no. 2895), anti-Bip (cat. no. 3177), anti-p-IRE1α (cat. no. ab124945), anti-IRE1α (cat. no. 3294), anti-p-PERK (cat. no. ab192591), anti-PERK (cat. no. 5683) and anti-GAPDH (cat. no. 5174; all antibodies were purchased from Cell Signaling Technology, Inc.; anti-p-IRE1α and p-PERK were from Abcam; 1:1,000) at 4°C overnight. After sufficient washing with PBST, the membrane was co-incubated with goat anti-rabbit or anti-mouse IgG/HRP (cat. nos. SE134 and SE131, respectively; 1:5,000; Beijing Solarbio Science & Technology Co., Ltd.) at room temperature for 2 h. Subsequently, ECL western blotting substrate (Beijing Solarbio Science & Technology Co., Ltd.) was added to detect the protein signal and GAPDH

was used as an internal reference. The relative protein intensity was determined using ImageJ (V1.8.0; NIH).

Intracellular ROS detection. After C-33A and HeLa cells were processed, the DCFH-DA fluorescent probe was diluted 1:1,000 in serum-free medium according to the manufacturer's instructions (Beijing Solarbio Science & Technology Co., Ltd.) and co-incubated with the cells at 37°C for 20 min (the final concentration of DCFH-DA was 10 µM). The cells were collected and detected via flow cytometry (BD FACS; BD Biosciences). The data were analyzed using FlowJo software (v10.10.0; FlowJo LLC).

Cell viability assay. A Cell Counting Kit-8 (CCK-8) (Beijing Solarbio Science & Technology Co., Ltd.) was used to detect the viability of the C-33A and HeLa cells. A total of 10³ cells were inoculated in 96-well plates and cultured overnight, after which different concentrations (0, 10, 20, 40, 80, 160 and 320 µM) of NCTD (Selleck Chemicals) were added to each well for treatment. Next, 10 µl of CCK-8 reagent was added to each well and incubated at 37°C for 2 h. The absorbance was measured at OD450 nm using a Thermo Scientific Multiskan MK3 Enzyme Mark Instrument (Thermo Fisher Scientific, Inc.). The 50% inhibitory concentration (IC₅₀) was calculated using GraphPad Prism 10 (Dotmatics).

To explore which type of cell death could be induced by NCTD in cervical cancer cells, the cells were preincubated with apoptosis inhibitor, z-VAD-FMK (ZVAD; 20 µM; MedChemExpress), the ER stress inhibitor 4-phenylbutyric acid (4-PBA; 10 mM; MedChemExpress), autophagy inhibitor, chloroquine (CQ; 20 µM; MedChemExpress), for 1 h at 37°C. Then, the cells were further treated with 40 µM NCTD for 37 h. After which, cell viability was determined as aforementioned.

Cell cycle assay. After C-33A and HeLa cells were processed, the cells were collected and washed well with PBS. Subsequently, a DNA Content Quantitation Assay (Cell Cycle; cat. no. CA1510; Beijing Solarbio Science & Technology Co., Ltd.) was used to detect cell cycle changes. Briefly, the prepared cell suspension was fixed with 70% pre-cooled ethanol for 2 h, and the cells were resuspended by adding 100 µl of RNase A solution to the cell pellet in a water bath at 37°C for 30 min. Subsequently, 400 µl of PI was added to each group of cells for 30 min at 4°C in the dark, after which the proteins were detected via flow cytometry (BD FACS; BD Biosciences). The data were analyzed using FlowJo software (v10.10.0; FlowJo LLC).

EdU staining. C-33A and HeLa cells were incubated with 100 µl of EdU staining solution (Wuhan Servicebio Technology Co., Ltd.) at 37°C for 2 h. After sufficient washing with PBS, the cells were fixed with 4% paraformaldehyde at room temperature for 30 min followed by addition of 100 µl of PBS containing 0.5% Triton X-100 at room temperature for 15 min. Finally, 10 µl of DAPI was added to the sections, which were incubated at room temperature for 10 min. Subsequently, the sections were blocked with an anti-fluorescence quenching sealer (Wuhan Servicebio Technology Co., Ltd.) and placed under a fluorescence microscope (Keyence Corporation) for observation.

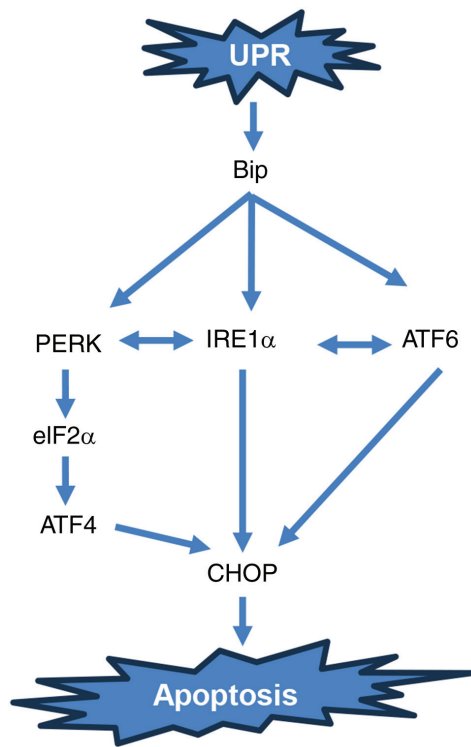


Figure 1. Schematic illustrating the important proteins involved in endoplasmic reticulum stress. UPR, unfolded protein response; PERK, protein kinase R-like ER kinase; IRE1 α , inositol-requiring enzyme 1 α ; ATF, activating transcription factor; eIF2 α , eukaryotic initiation factor 2 α ; CHOP, C/EBP homologous protein.

DNA damage assay. The effect of NCTD on DNA damage in C-33A and HeLa cells in the present study was assessed via a DNA damage assay kit (cat. no. C2035S; Beyotime Institute of Biotechnology), and the specific steps were carried out according to the manufacturer's instructions. The relative fluorescence density was observed under a fluorescence microscope (Keyence Corporation).

Intracellular Ca^{2+} level assay. An intracellular Ca^{2+} Assay Kit (F04 method; cat. no. HR8229; Beijing Biolab Technology Co., Ltd.) was used to detect changes in the intracellular calcium ion concentration. Briefly, C-33A and HeLa cells were washed thoroughly with HBSS, and F04 staining working solution was subsequently added according to the manufacturer's instructions. Afterwards, the cells were incubated at 37°C for 30 min before the fluorescence intensity of Ca^{2+} was detected under a fluorescence microscope (Keyence Corporation).

Mitochondrial membrane potential (MMP) assay. MMP detection was performed using a Mitochondrial Membrane Potential Assay Kit with JC-1 (Beijing Solarbio Science & Technology Co., Ltd.). C-33A and HeLa cells were inoculated in six-well plates, and after treatment with 40 μM NCTD at 37°C for 24 h, the cells were washed three times with PBS. Subsequently, the cells were collected, stained according to the manufacturer's instructions and recorded under a fluorescence microscope (Keyence Corporation). When the MMP is high, JC-1 aggregates in the matrix of mitochondria and forms polymers, which can produce red

fluorescence; when the mitochondrial membrane potential is low, JC-1 cannot aggregate in the matrix of mitochondria, and at this time, JC-1 is a monomer that can produce green fluorescence.

Tumor model in nude mice. The present study was approved by The Animal Ethics Committee at Tongliao City Hospital (Tongliao, China; approval no. 2023-TLAJ34). Male nude mice aged 6-7 weeks (20 \pm 4 g) used in the present study and were purchased from SPF (Beijing) Biotechnology, Co., Ltd. All mice were housed in a temperature-(20-24°C) and humidity-controlled (45-55%) environment. A 12/12 h light/dark cycle was maintained in the animal housing rooms. All mice had free access to food and water. A total of 10⁶ HeLa cells (100 μl) were injected subcutaneously into the nude mice through the right lower abdomen to construct the nude mouse subcutaneous tumor model. Subsequently, the model mice were randomly divided into 2 groups (n=8/group) and given subcutaneous injections of PBS or 3 mg/kg NCTD every 2 days for 5 consecutive treatments, after which the body weights of the mice and the growth of the subcutaneous tumors were recorded. In order to anesthetize the mice, 4% isoflurane was used. The mice were deeply anesthetized when they breathed evenly, had no splinting pain reflex and had no corneal reflex. Subsequently, cervical dislocation was used to execute the mice, and the mice were judged to be dead when their heartbeat stopped. At the end of treatment, the subcutaneous tumor tissues of the mice in each group were removed and weighed, and the tumor tissues were subjected to pathological section analysis.

H&E staining. Tissue specimens were fixed in 4% paraformaldehyde (Beijing Solarbio Science & Technology Co., Ltd.) at room temperature for 24 h. The fixed tissues were then fully dehydrated and paraffin embedded. Sections were cut into 5 μm sections, which were then baked and deparaffinized at 70°C. Sections were stained with hematoxylin staining solution (H&E; Beijing Solarbio Science & Technology Co., Ltd.) as well as 0.5% eosin (Beijing Solarbio Science & Technology Co., Ltd.) for 2 min at room temperature, and after gradient dehydration with ethanol and treatment with xylene, the sections were oven-dried and treated with neutral gum (Beijing Solarbio Science & Technology Co., Ltd.). The pathological morphology of the tissues was observed under a light microscope (Keyence Corporation) and recorded.

Immunohistochemistry (IHC). Tissue specimens were fixed in 4% paraformaldehyde (Beijing Solarbio Science & Technology Co., Ltd.) at room temperature for 24 h. The fixed tissues were then fully dehydrated and paraffin embedded. Sections were cut into 5 μm sections, which were then baked and deparaffinized at 70°C. After that, the sections were incubated with 10% BSA at 37°C for 1 h, anti-CHOP (cat. no. 2895; 1:50; CST Biological Reagents Co., Ltd.) or anti-Bip (cat. no. 3177; 1:50; CST Biological Reagents Co., Ltd.) were added to the sections and incubated at 4°C overnight. After rinsing with PBS for 3 h, 60 μl of biotin-labeled Goat Anti-Mouse or Anti-Rabbit IgG (H+L; cat. nos. A0286 and A0277, respectively; 1:50; Beyotime Institute of Biotechnology) were added to the sections, which were incubated at 37°C for 1 h. Then, the sections were color developed by adding an appropriate

amount of DAB Horseradish Peroxidase Color Development Kit (cat. no. P0202; Beyotime Institute of Biotechnology) for 10 min at room temperature, washed with tap water three times, and immediately stained with hematoxylin stain for 5 min at room temperature. After sufficient dehydration and transparency, the sections were closed with neutral gum (Beijing Solarbio Science & Technology Co., Ltd.) and subsequently observed under a microscope (Keyence Corporation).

Hematoxylin and Eosin Staining Kit (cat. no. C0105S, Beyotime, Shanghai, China) was used for the detection of liver and kidney pathological changes. After the slides were prepared as described above, the slides were stained with hematoxylin at room temperature for 5 min, rinsed in tap water, and continued to be stained with eosin for 1 min. Sections were sealed according to the above procedure and observed under the microscope (Keyence Corporation).

Statistical analysis. All the data in the present study are expressed as the mean \pm standard deviation. GraphPad Prism 10 (Dotmatics) was used for statistical analysis. Comparisons between two groups were made using unpaired Student's *t*-tests, while comparisons between more than three groups were made using one-way ANOVA followed by post hoc analysis (Tukey's HSD). $P < 0.05$ was considered to indicate a statistically significant difference.

Results

NCTD inhibits the proliferation of cervical cancer cells. Whether NCTD inhibited the proliferation of cervical cancer cells was first tested. NCTD reduced the viability of C-33A and HeLa cells in a concentration-dependent manner (Fig. 2A and B). The IC_{50} values of these compounds in C-33A and HeLa cells were 45.12 and 44.02 μ M, respectively. Therefore, 40 μ M NCTD was selected for subsequent experiments. Next, the effect of NCTD on the proliferation of cervical cancer cells was detected by EdU staining. Compared with that in the control group, the EdU staining of C-33A and HeLa cells was attenuated after NCTD treatment (Fig. 2C and D). Flow cytometry revealed that NCTD significantly blocked the cell cycle progression of C-33A and HeLa cells, as evidenced by an increase in the cell population in G1 phase and a decrease in the cell population in S+G2 phase (Fig. 2E and F). These results suggested that NCTD can inhibit the malignant proliferation of cervical cancer cells.

ER stress inhibitor 4-phenylbutyric acid reverses NCTD-induced cervical cancer cell death. The mechanism by which NCTD actually causes cervical cancer cell death was further explored. The NCTD-induced reduction in the viability of C-33A and HeLa cells was reversed by the apoptosis inhibitor, ZVAD and the ER stress inhibitor, 4-PBA, but the autophagy inhibitor CQ had no significant effect (Fig. 3A and B). Compared with apoptosis inhibitors, 4-PBA appeared to have a more pronounced ability to reverse the decrease in NCTD-cell viability. Additionally, the intracellular Ca^{2+} concentration was examined. Compared with those in the controls, the Ca^{2+} levels in the NCTD-treated C-33A and HeLa cells were significantly elevated (Fig. 3C and D). Moreover, ZVAD and 4-PBA

reversed the NCTD-induced increase in Ca^{2+} levels, but CQ did not have this effect (Fig. 3C and D). These results suggested that ER stress may play an important role in the NCTD-induced decrease in the proliferative capacity of cervical cancer cells.

ER stress inhibitor 4-PBA attenuates NCTD-induced MMP reduction in cervical cancer cells. Mitochondrial damage is an important step in cell death. Therefore, the effect of NCTD on ROS accumulation in cervical cancer cells was also examined. Flow cytometry assays showed that, compared with the control treatment, NCTD treatment significantly increased the level of ROS in C-33A and HeLa cells, while 4-PBA pre-treatment attenuated NCTD-induced ROS accumulation (Fig. 4A and B). Unlike in the control group, in the NCTD treatment group, the MMP was significantly decreased, as evidenced by an increase in the level of mono-JC-1. The NCTD-induced decrease in the MMP was ameliorated to some extent by 4-PBA pre-treatment (Fig. 4C and D). These results suggested that the NCTD-induced decrease in mitochondrial function can be ameliorated by 4-PBA, an inhibitor of ER stress.

NCTD induces apoptosis in cervical cancer cells via the ATF4-CHOP pathway. Next, the effect of NCTD on the ER stress-related apoptotic pathway was examined. NCTD increased the protein expression of Bip, ATF4 and CHOP in a concentration-dependent manner in C-33A and HeLa cells (Fig. 5A and B). These results suggested that NCTD could induce apoptosis in cervical cancer cells by activating ER stress.

ER stress inhibitor 4-PBA reverses NCTD-induced IRE1 α and PERK activation. In addition to examining the effects of ATF6, the effects of NCTD on the activation of two other UPR pathways, IRE1 α and PERK were examined. NCTD significantly elevated the phosphorylation levels of IRE1 α and PERK in cervical cancer cells, whereas 4-PBA pre-treatment significantly reduced the NCTD-induced increase in p-IRE1 α and p-PERK (Fig. 6A and B). Moreover, NCTD increased the IF intensity of γ -H2A in cervical cancer cells, while 4-PBA attenuated the IF intensity of γ -H2A (Fig. 6C and D). These results suggested that NCTD-induced ER stress and DNA damage in cervical cancer cells can be reversed by 4-PBA.

NCTD attenuates tumor growth in mice in vivo. Next, whether NCTD attenuated tumor growth *in vivo* was tested. NCTD did not have side effects on the liver or kidney, indicating that it is safe for these organs (Fig. 7A and B). NCTD significantly reduced the weight and volume of the tumors (Fig. 7C and D). Additionally, the expression of CHOP and Bip in the tumor tissues of the mice was detected by IHC (Fig. 7E and F). Compared with those in the control group, the levels of CHOP and Bip in mouse tumor tissues were greater in the NCTD group. Moreover, three UPR-related pathways, namely, the ATF6, p-IRE1 α /IRE1 α and p-PERK/PERK pathways, were activated by NCTD in tumor tissues (Fig. 7G). These results suggested that NCTD can inhibit tumor growth in mice *in vivo*.

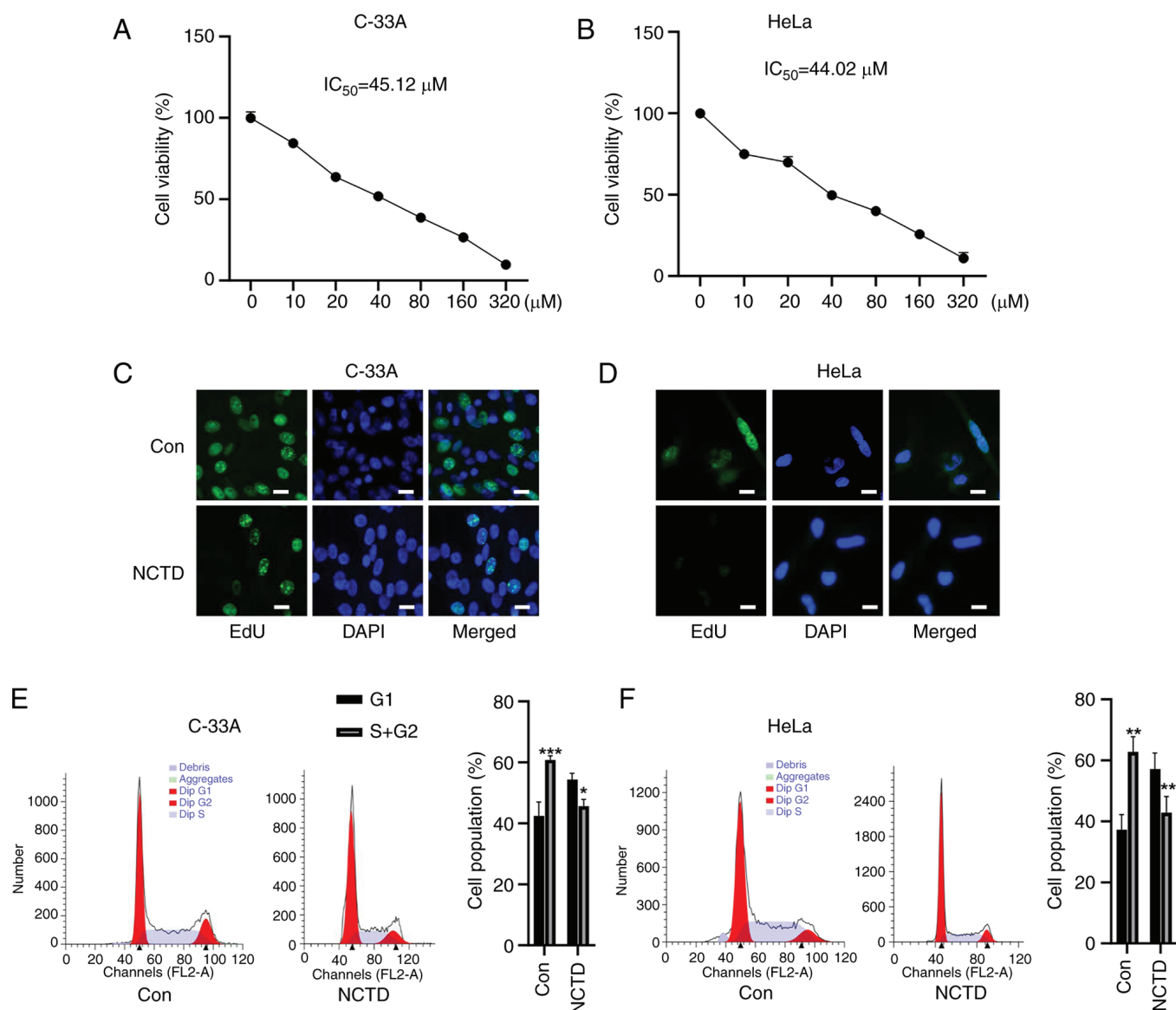


Figure 2. NCTD reduced the proliferative ability of cervical cancer cells. CCK-8 analysis showed that NCTD reduced the viability of (A) C-33A and (B) HeLa cells in a concentration-dependent manner. EdU staining confirmed that NCTD attenuated the proliferative ability of (C) C-33A and (D) HeLa cells. Flow cytometry revealed that NCTD significantly caused cell cycle arrest in (E) C-33A and (F) HeLa cells. * $P < 0.05$, ** $P < 0.01$ and *** $P < 0.001$ vs. Con. Con, control; NCTD, norcantharidin.

Discussion

ER stress is a double-edged sword (17). On the one hand, ER stress is important for tumor microenvironmental homeostasis and tumor growth inhibition; on the other hand, sustained ER stress can initiate multiple signaling pathways to promote tumor cell death (18). Therefore, targeting ER stress-related signals to regulate tumor cell death may constitute a potential strategy for tumor treatment and intervention (18). NCTD is a novel synthetic antitumor drug with clear antitumor and leukocyte-enhancing effects (19), but its efficacy in treating cervical cancer alone has not been reported.

In the present study, to the best of our knowledge, for the first time it was found that NCTD significantly inhibited the proliferation of cervical cancer cells in a concentration-dependent manner. Further studies revealed that the ER stress inhibitor 4-PBA and the apoptosis inhibitor ZVAD could reverse the

NCTD-induced reduction in cervical cancer cell viability to some extent. Disturbed Ca^{2+} homeostasis is also a major manifestation of ER stress (17). Therefore, the effect of NCTD on Ca^{2+} levels was evaluated. NCTD increased Ca^{2+} levels in cervical cancer cells, whereas 4-PBA reduced NCTD-induced Ca^{2+} elevation, suggesting that ER stress is likely involved in the NCTD-mediated reduction in cervical cancer cell viability.

ROS can react directly with proteins and their precursors, affecting protein assembly and modification and leading to a large accumulation of misfolded proteins as well as unfolded proteins in the ER, which is an important factor in inducing ER stress (20). It was clarified that NCTD can significantly promote ROS generation in cervical cancer cells and that this ROS accumulation is positively associated with a decrease in cervical cancer cell viability. Mitochondria and the ER are structurally related, and the two can be directly connected at the outer mitochondrial membrane and form transfer channels

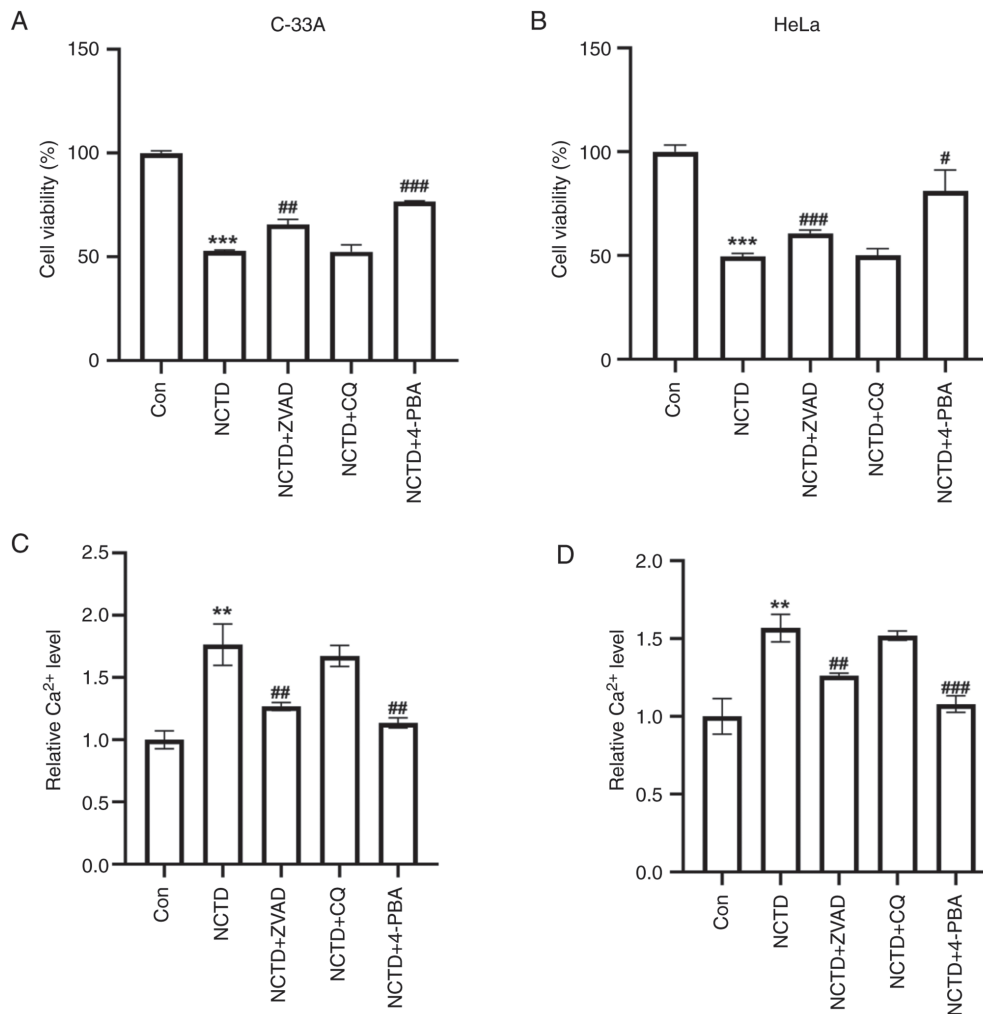


Figure 3. ER stress may play an important role in the NCTD-induced decrease in the proliferative capacity of cervical cancer cells. CCK-8 analysis showed that ZVAD and 4-PBA reversed the NCTD-induced decrease in the viability of (A) C-33A and (B) HeLa cells. (C) ZVAD and (D) 4-PBA partially abolished the NCTD-induced decrease in the viability of C-33A and HeLa cells. NCTD-induced an elevation of Ca²⁺ levels. **P<0.01, ***P<0.001 vs. Con; #P<0.05, ##P<0.01, ###P<0.001 vs. NCTD. Con, control; NCTD, norcantharidin; ZVAD, z-VAD-FMK; 4-PBA, 4-phenylbutyric acid.

to facilitate the transfer of Ca²⁺ between the ER and mitochondria to regulate mitochondrial metabolic homeostasis and apoptotic pathways (20,21). Therefore, mitochondria are also important regulatory target organelles of ER stress. In the present study, it was found that NCTD disrupted mitochondrial function, which was manifested by increased ROS generation and decreased MMP, suggesting that mitochondria are important targets through which NCTD kills cervical cancer cells. An inhibitor of ER stress, 4-PBA, reversed the disruption of mitochondrial function induced by NCTD, suggesting that NCTD affects mitochondrial function in cervical cancer cells by regulating ER stress.

ER stress refers to a series of cellular adaptive responses and regulatory pathways caused by the disruption of protein folding and modification in the ER when cells are subjected to a variety of physiological and pathological factors, as well as nutritional deficiencies (6,22). ER stress promotes cell survival by activating a series of adaptive mechanisms called the UPR, which provides an improved microenvironment for the survival of tumor cells (23). However, sustained ER stress can directly regulate cell death, providing an important strategy for selective antitumor therapy (7,24).

ER stress can activate intracellular PERK, IRE1 α and ATF6, which in turn promotes the transcription of the apoptosis-related protein CHOP (10,24). In the present study, it was shown that NCTD can increase the expression of the apoptosis-related proteins Bip, ATF4 and CHOP in a concentration-dependent manner. In addition, it was also found that NCTD significantly increased the phosphorylation of PERK and IRE1 α and that the ER-specific inhibitor 4-PBA significantly ameliorated the effects of NCTD on ER stress-related proteins in cervical cancer cells, suggesting that NCTD regulates tumor cell apoptosis by activating ER stress in cervical cancer cells. Although HPV is the main cause of cervical cancer, there are still some cervical cancers that are not caused by HPV infection (25). To investigate whether NCTD has a generalized inhibitory effect on different types of cervical cancer, two cell lines, an HPV-negative C-33A cell line and an HPV-positive HeLa cell line, were used in the present study. The data showed that NCTD significantly induced apoptosis in cervical cancer cells through the activation of ER stress in both cell lines. Accordingly, it was hypothesized that NCTD has a therapeutic effect on different types of cervical cancer.

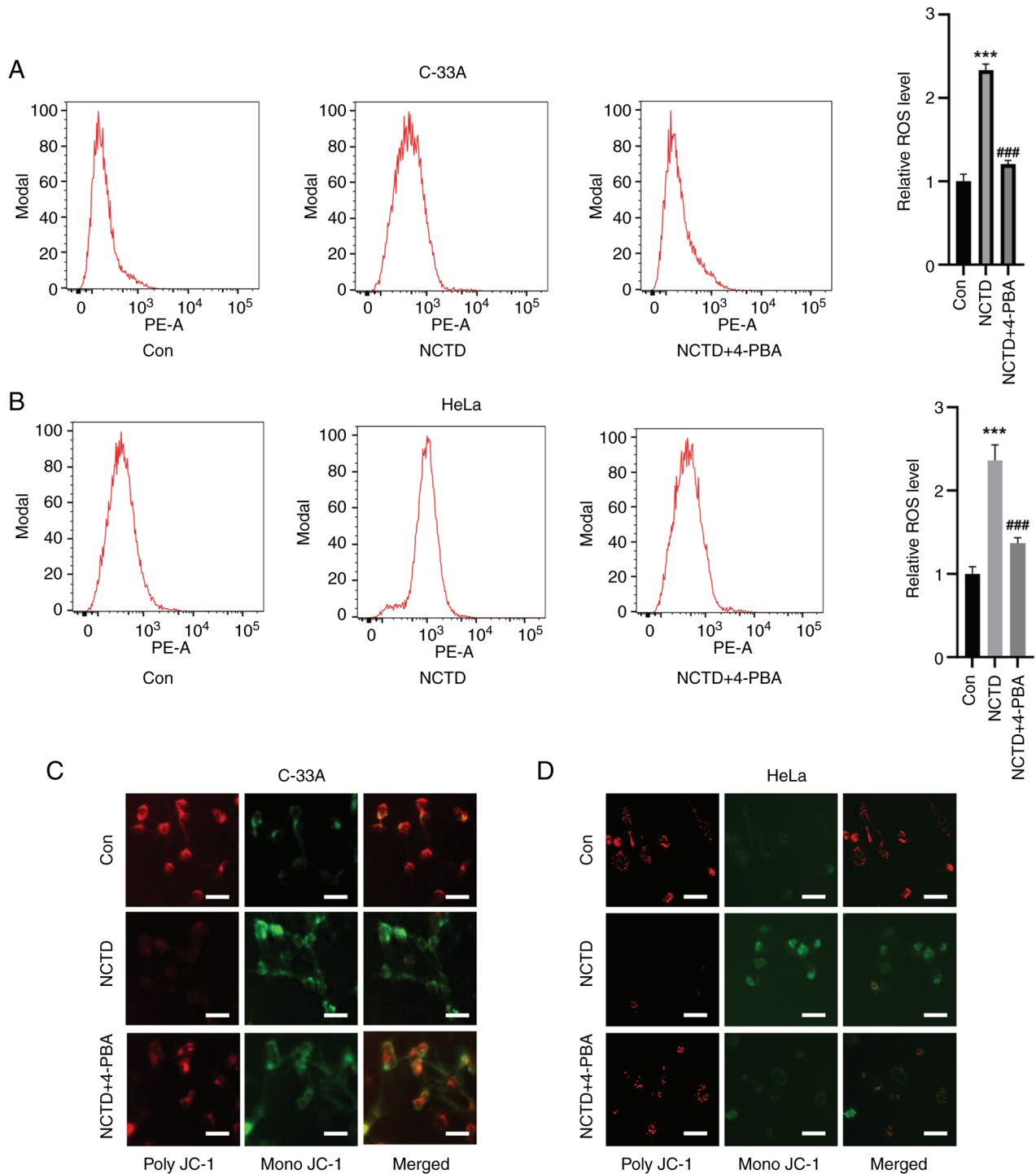


Figure 4. NCTD-induced decrease in mitochondrial function can be ameliorated by 4-PBA, an inhibitor of ER stress. Flow cytometry revealed that the NCTD-induced increase in ROS could be reversed by 4-PBA pre-treatment in (A) C-33A and (B) HeLa cells. JC-1 staining showed that the NCTD-induced increase in the mono-JC-1 concentration could be mitigated by 4-PBA in (C) C-33A and (D) HeLa cells. *** $P < 0.001$; ### $P < 0.001$ vs. NCTD. Con, control; NCTD, norcantharidin; 4-PBA, 4-phenylbutyric acid.

In vivo experiments showed that NCTD significantly inhibited the growth of subcutaneous tumors in mice. H&E staining showed that NCTD treatment reduced the malignant proliferation of cells in mouse tumor tissues. Moreover, the expression of ER stress-related molecules and apoptosis-related proteins increased significantly after NCTD treatment. Therefore, *in vivo* experiments demonstrated that NCTD could induce ER stress to inhibit tumor growth. It was also noted that NCTD

increased the vacuolization of xenograft tumors in nude mice. It was hypothesized that NCTD induces ER stress and expansion, which leads to the emergence and fusion of ER-derived vacuoles. ER expansion is a typical feature of paraptosis (26). Thus, NCTD induced sustained ER pressure and inhibited the malignant progression of cervical cancer. However, whether NCTD is an ER stress inducer with specific therapeutic effects on cervical cancer cells remains to be explored.

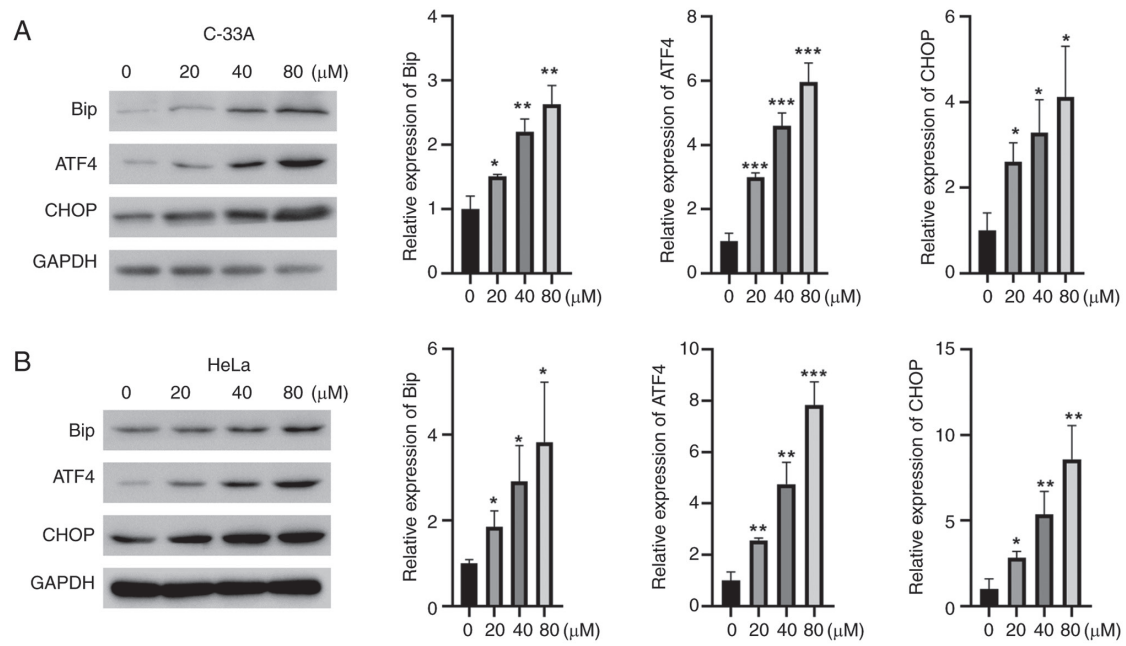


Figure 5. NCTD can induce apoptosis in cervical cancer cells by activating endoplasmic reticulum stress. In (A) C-33A and (B) HeLa cells, NCTD increased the protein expression of Bip, ATF4 and CHOP in a concentration-dependent manner. * $P < 0.05$, ** $P < 0.01$, *** $P < 0.001$ vs. Con. Con, control; NCTD, norcantharidin; ATF4, activating transcription factor 4; CHOP, C/EBP homologous protein.

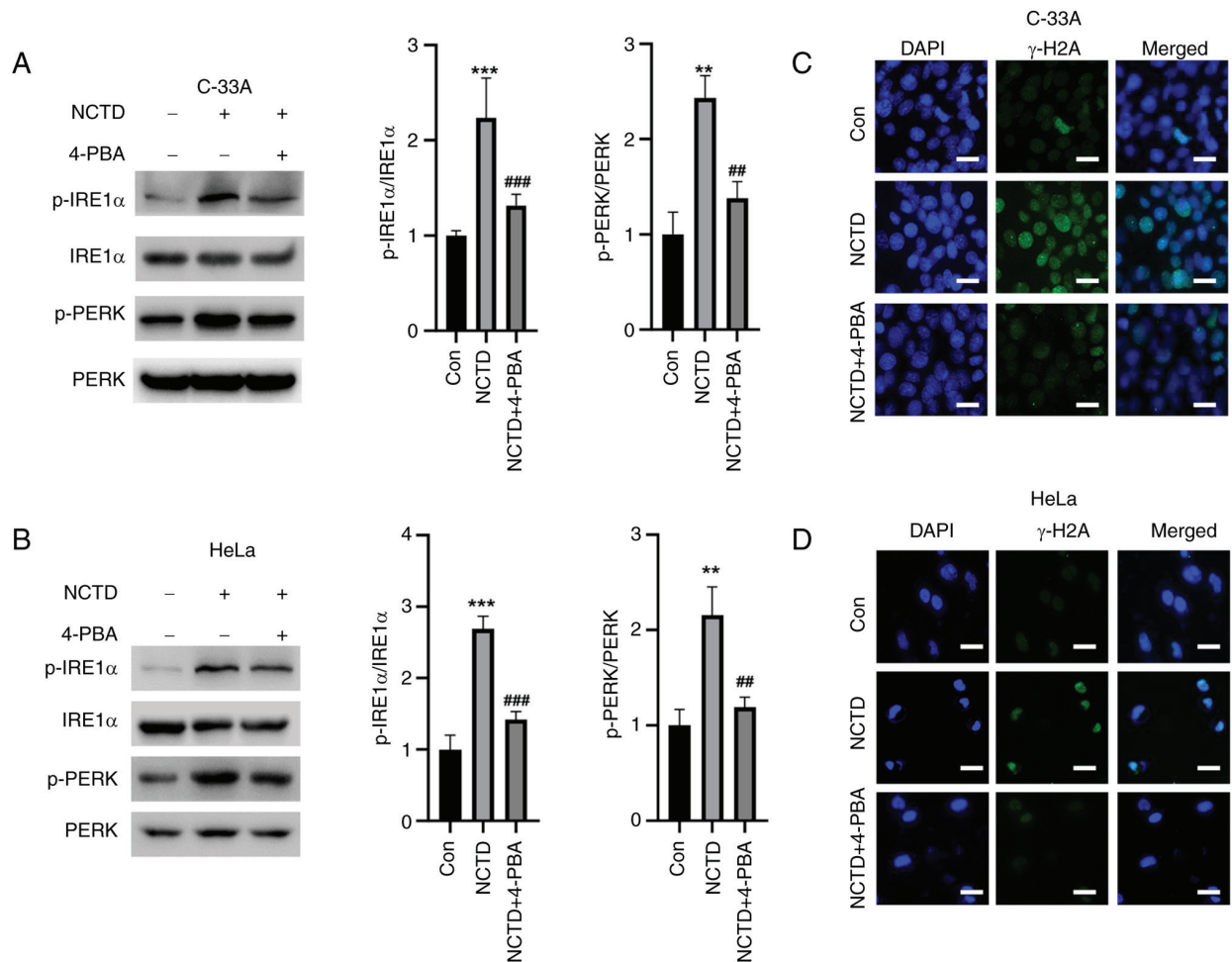


Figure 6. Endoplasmic reticulum stress inhibitor 4-PBA reversed NCTD-induced IRE1α and PERK activation. Western blotting assays revealed that 4-PBA pre-treatment significantly reduced the NCTD-induced increase in p-IRE1α and p-PERK in (A) C-33A and (B) HeLa cells. In (C) C-33A and (D) HeLa cells, 4-PBA attenuated NCTD-induced DNA damage. ** $P < 0.01$, *** $P < 0.001$ vs. Con; ## $P < 0.01$, ### $P < 0.001$ vs. NCTD. Con, control; NCTD, norcantharidin; PERK, protein kinase R-like ER kinase; IRE1α, inositol-requiring enzyme 1α; 4-PBA, 4-phenylbutyric acid; p-, phosphorylated.

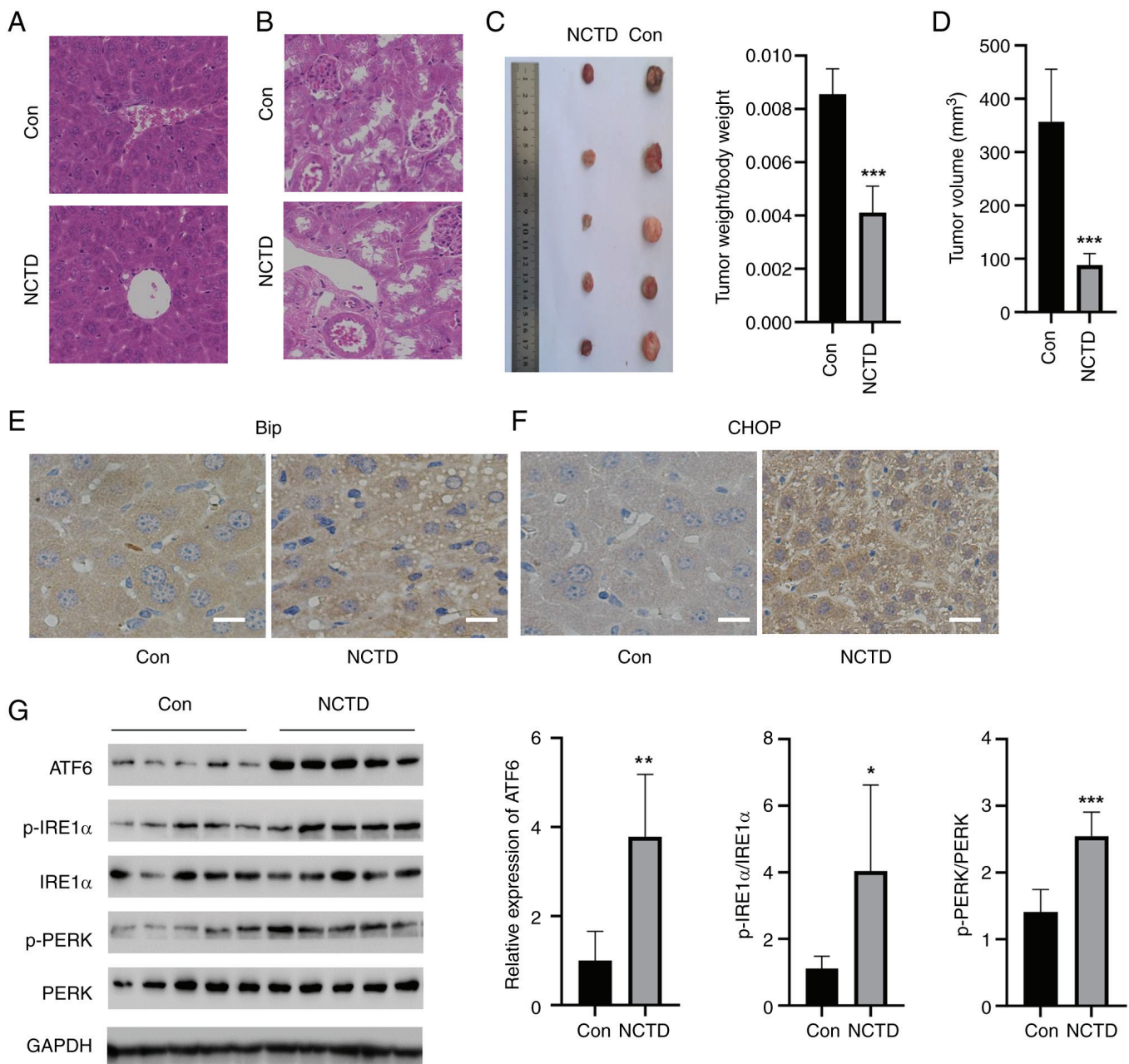


Figure 7. NCTD attenuated tumor growth in mice *in vivo*. H&E staining showed that NCTD did not have side effects on the (A) liver or (B) kidney. NCTD significantly reduced the (C) weight (Left, tumor images; Right, tumor weight) and (D) volume of the tumors. Immunohistochemical staining showed that NCTD significantly increased the levels of (E) Bip and (F) CHOP in the tumor tissues of mice. (G) NCTD increased the levels of ATF6, p-IRE1 α /IRE1 α and p-PERK/PERK in tumor tissues. * $P < 0.05$, ** $P < 0.01$, *** $P < 0.001$ vs. Con. Con, control; NCTD, norcantharidin; PERK, protein kinase R-like ER kinase; IRE1 α , inositol-requiring enzyme 1 α ; p-, phosphorylated; ATF6, activating transcription factor 6; CHOP, C/EBP homologous protein.

The following limitations were also present in the present study. The antitumor effects of NCTD have been widely reported, but NCTD also plays a wide range of roles in other diseases. For example, NCTD ameliorates renal tubulointerstitial fibrosis by blocking TGF- β 1/Smad signaling as well as the NF- κ B pathway (27). In lipopolysaccharide-induced macrophages, NCTD downregulates hepcidin expression through the inhibition of IL-6/JAK2/STAT3 signaling, resulting in a reduction in iron in the mouse liver and spleen (28). In a mouse model of systemic lupus erythematosus, NCTD blockade of STAT3 signaling inhibited Th17 cell differentiation and attenuated the inflammatory response (29). Therefore, it is not known whether NCTD curbs

the development of cervical cancer through other signaling pathways and thus, this requires further exploration. In future studies, whether NCTD inhibits cervical cancer through other molecular mechanisms will be investigated. Moreover, to promote the potential clinical application of NCTD, the number of samples in animal experiments will be increased to determine its efficacy and safety.

In conclusion, NCTD regulates cell death by inducing the ER stress pathway in cervical cancer cells. Therefore, NCTD could be a potential ER stress inducer and thus a potential strategy for anticancer cancer therapy. The present study revealed to the best of our knowledge for the first time that NCTD is a potential therapeutic agent

for the treatment of cervical cancer, but its actual clinical application needs to be confirmed by additional experiments.

Acknowledgments

Not applicable.

Funding

This work was supported by Natural Science Foundation of Inner Mongolia Autonomous Region (grant no. 2019BS08001).

Availability of data and materials

The data generated in the present study may be requested from the corresponding author.

Authors' contributions

ZZ performed the experiments and analyzed the data. BS, JL PB, YS, YL performed the animal experiments. ZZ designed the experiment, analyzed the data and gave final approval of the version to be published. ZZ, BS, JL PB, YS and YL confirm the authenticity of all the raw data. All authors read and approved the final version of the manuscript.

Ethics approval and consent to participate

The present study was approved by The Animal Ethics Committee at Tongliao City Hospital (approval no. 2023-TLAJ34; Tongliao, China).

Patient consent for publication

Not applicable.

Competing interests

The authors declare that they have no competing interests.

References

- Buskwofie A, David-West G and Clare CA: A review of cervical cancer: Incidence and disparities. *J Natl Med Assoc* 112: 229-232, 2020.
- Kusakabe M, Taguchi A, Sone K, Mori M and Osuga Y: Carcinogenesis and management of human papillomavirus-associated cervical cancer. *Int J Clin Oncol* 28: 965-974, 2023.
- Revathidevi S, Murugan AK, Nakaoka H, Inoue I and Munirajan AK: APOBEC: A molecular driver in cervical cancer pathogenesis. *Cancer Lett* 496: 104-116, 2021.
- Hill EK: Updates in cervical cancer treatment. *Clin Obstet Gynecol* 63: 3-11, 2020.
- Mayadev JS, Ke G, Mahantshetty U, Pereira MD, Tarnawski R and Toita T: Global challenges of radiotherapy for the treatment of locally advanced cervical cancer. *Int J Gynecol Cancer* 32: 436-445, 2022.
- Chen X and Cubillos-Ruiz JR: Endoplasmic reticulum stress signals in the tumor and its microenvironment. *Nat Rev Cancer* 21: 71-88, 2021.
- Marciniak SJ, Chambers JE and Ron D: Pharmacological targeting of endoplasmic reticulum stress in disease. *Nat Rev Drug Discov* 21: 115-140, 2022.
- Qi Z and Chen L: Endoplasmic Reticulum Stress and Autophagy. *Adv Exp Med Biol* 1206: 167-177, 2019.
- Ren J, Bi Y, Sowers JR, Hetz C and Zhang Y: Endoplasmic reticulum stress and unfolded protein response in cardiovascular diseases. *Nat Rev Cardiol* 18: 499-521, 2021.
- Groenendyk J, Agellon LB and Michalak M: Calcium signaling and endoplasmic reticulum stress. *Int Rev Cell Mol Biol* 363: 1-20, 2021.
- Oakes SA: Endoplasmic reticulum stress signaling in cancer cells. *Am J Pathol* 190: 934-946, 2020.
- Chen X, Shi C, He M, Xiong S and Xia X: Endoplasmic reticulum stress: Molecular mechanism and therapeutic targets. *Signal Transduct Target Ther* 8: 352, 2023.
- Tang Y, Zhou X, Cao T, Chen E, Li Y, Lei W, Hu Y, He B and Liu S: Endoplasmic reticulum stress and oxidative stress in inflammatory diseases. *DNA Cell Biol* 41: 924-934, 2022.
- Deng L and Tang S: Norcantharidin analogs: A patent review (2006-2010). *Expert Opin Ther Pat* 21: 1743-53, 2011.
- Liu Z, Li B, Cao M and Jiang J: Norcantharidin triggers apoptotic cell death in non-small cell lung cancer via a mitophagy-mediated autophagy pathway. *Ann Transl Med* 9: 971, 2021.
- Shi X, Chen S, Zhang Y, Xie W, Hu Z, Li H, Li J, Zhou Z and Tan W: Norcantharidin inhibits the DDR of bladder cancer stem-like cells through cdc6 degradation. *Onco Targets Ther* 12: 4403-4413, 2019.
- Xu D, Liu Z, Liang MX, Fei YJ, Zhang W, Wu Y and Tang JH: Endoplasmic reticulum stress targeted therapy for breast cancer. *Cell Commun Signal* 20: 174, 2022.
- Zhao T, Du J and Zeng H: Interplay between endoplasmic reticulum stress and noncoding RNAs in cancer. *J Hematol Oncol* 13: 163, 2020.
- Zhai BT, Sun J, Shi YJ, Zhang XF, Zou JB, Cheng JX, Fan Y, Guo DY and Tian H: Review targeted drug delivery systems for norcantharidin in cancer therapy. *J Nanobiotechnology* 20: 509, 2022.
- Wadgaonkar P and Chen F: Connections between endoplasmic reticulum stress-associated unfolded protein response, mitochondria, and autophagy in arsenic-induced carcinogenesis. *Semin Cancer Biol* 76: 258-266, 2021.
- Senft D and Ronai ZA: UPR, autophagy, and mitochondria crosstalk underlies the ER stress response. *Trends Biochem Sci* 40: 141-8, 2015.
- Wiseman RL, Mesgarzadeh JS and Hendershot LM: Reshaping endoplasmic reticulum quality control through the unfolded protein response. *Mol Cell* 82: 1477-1491, 2022.
- Hetz C, Zhang K and Kaufman RJ: Mechanisms, regulation and functions of the unfolded protein response. *Nat Rev Mol Cell Biol* 21: 421-438, 2020.
- Hetz C: The unfolded protein response: Controlling cell fate decisions under ER stress and beyond. *Nat Rev Mol Cell Biol* 13: 89-102, 2012.
- Fernandes A, Viveros-Carreño D, Hoegl J, Ávila M and Pareja R: Human papillomavirus-independent cervical cancer. *Int J Gynecol Cancer* 32: 1-7, 2022.
- Seo MJ, Lee DM, Kim IY, Lee D, Choi MK, Lee JY, Park SS, Jeong SY, Choi EK and Choi KS: Gambogic acid triggers vacuolization-associated cell death in cancer cells via disruption of thiol proteostasis. *Cell Death Dis* 10: 187, 2019.
- Li Y, Ge Y, Liu FY, Peng YM, Sun L, Li J, Chen Q, Sun Y and Ye K: Norcantharidin, a protective therapeutic agent in renal tubulointerstitial fibrosis. *Mol Cell Biochem* 361: 79-83, 2012.
- Zheng J, Qian ZM, Sun YX and Bao YX: Downregulation of hepcidin by norcantharidin in macrophage. *Nat Prod Res* 38: 673-678, 2024.
- Du LJ, Feng YX, He ZX, Huang L, Wang Q, Wen CP and Zhang Y: Norcantharidin ameliorates the development of murine lupus by inhibiting the generation of IL-17 producing cells. *Acta Pharmacol Sin* 43: 1521-1533, 2022.



Copyright © 2024 Zhang et al. This work is licensed under a Creative Commons Attribution-NonCommercial-NoDerivatives 4.0 International (CC BY-NC-ND 4.0) License.